

Measurement of the point spread function of a soft X-ray microscope by single pixel exposure of photoresists

Adam F. G. Leontowich,^a Tolek Tyliczszak^b and Adam P. Hitchcock*^a

^aBrockhouse Institute for Materials Research,
McMaster University, Hamilton, ON, Canada L8S 4M1

^bAdvanced Light Source, Lawrence Berkeley National Laboratory,
1 Cyclotron Road, Berkeley, CA, USA, 94720

ABSTRACT

The monochromatic zone plate focused soft X-rays of scanning transmission X-ray microscopes (STXM) can be used to directly write patterns in common photoresists, analogous to lithography with a focused electron or ion beam. A radiation damage spreading phenomenon when patterning with high doses was recently determined to be due to the point spread function of the optical system (Leontowich et al., *Applied Physics A: Materials Science and Processing* 103, 1 (2011)). We have used this phenomenon to measure the point spread function of three different STXMs by making a series of single pixel exposures in a photoresist at focus over a controlled dose range. Our results suggest this measurement is sensitive to zone plate aberrations; thus, it could be valuable feedback for optimizing zone plate fabrication schemes and STXM performance.

Keywords: Zone plate, point spread function, X-ray lithography, radiation damage, aberrations

*aph@mcmaster.ca; phone 1 905 525-9140 x24749; fax 1 905 521-2773

1. INTRODUCTION

The current generation of soft X-ray (60 – 2500 eV) scanning transmission X-ray microscopes (STXM) employ Fresnel zone plate (ZP) lenses^{1,2} to focus sufficiently coherent soft X-rays into a tightly focused probe. The sample is then positioned at the focal point and x-y raster scanned while the transmitted signal is acquired to form images at specific photon energies.^{1,3} In addition, near edge X-ray absorption fine structure (NEXAFS) spectra can be measured by recording image sequences over the energy range of interest.^{2,5} STXM is an excellent instrument for NEXAFS spectromicroscopy and has been used extensively to characterize many diverse types of samples with high spatial and spectral resolution.^{4,5}

Advancements in ZP fabrication via electron beam lithography^{6,7} have steadily improved the spatial resolution of STXMs. The state-of-the-art is now 10 nm, and routine spot sizes (as defined by the Rayleigh criterion^{1,8}) are ~30 nm. Soft X-ray STXMs can provide an intensity of $10^7 - 10^8$ photons/sec in the focal spot; typical absorbed dose rates are in the 100 - 1000 MGy/s range, assuming an optical density of 1. The absorbed dose can be large enough to induce a variety of changes to the sample,⁹ and fundamentally limits useful spatial resolution.¹⁰ For sensitive samples, this can result in a race to capture spectroscopic information before it is modified by the effects of radiation.

Intense tightly focused probes of ionizing radiation (most commonly electrons or ions) are used extensively to direct write pattern materials for micro and nanofabrication. Zhang et al.¹¹ were the first to demonstrate sub-micron direct write patterning with focused X-rays by operating a STXM in a manner analogous to an electron beam writer. Since that initial work, several groups have investigated ZP focused X-rays for direct write patterning and lithography.¹²⁻¹⁵ A common observation in these experiments is that the minimum feature sizes created when patterning with ZP focused soft X-rays were always larger than the Rayleigh resolution predicted from the ZP properties and measured by imaging high contrast resolution test patterns. Further experiments revealed that feature sizes were dose dependent, implying the existence of an exposure spread mechanism which is in many ways similar to the proximity effect observed in electron beam lithography.¹⁶ We have recently shown¹⁷ that the exposure spread mechanism is caused by instrument properties, namely, the point spread function (PSF) of the optical system, i.e. the distribution of radiation intensity about the focal axis. This was experimentally determined by making repeated, long dwell time, single point exposures in photoresists

positioned at the focal plane of the ZP, and observing asymmetric yet fully reproducible patterns which delineate the spatial extent of the PSF.

In this report, we use thin films of poly(methyl methacrylate) (PMMA) positioned in the focal plane of the ZP to record precisely where X-rays impinge, analogous to photographic film. Soft X-rays cause primarily main chain scission in PMMA at low dose, and crosslinking at high dose. The lower molecular weight areas are then revealed by a wet chemical development step. We have previously determined that PMMA is fully removed from the substrate if it receives a dose of 1 MGy, but even a dose of 0.1 MGy will result in partial removal of material.¹⁷ The developed films are then read out using an atomic force microscope (AFM). Here, we explore more fully the relationship between developed pattern features, properties of the ZP, and its illumination. We have extracted full PSFs from a series of single pixel exposures in PMMA, at focus, over a controlled dose range. We have observed partial Airy patterns with three different STXMs. We have not yet observed the fully symmetric Airy pattern that theory predicts should be formed with a high quality zone plate and optimal illumination. We hypothesize some reasons for this, and discuss planned experiments intended to isolate the source(s) of the asymmetry.

2. METHODOLOGY

2.1 Sample preparation

Thin films (~100 nm) of poly(methyl methacrylate) (PMMA) (M_w : 315 000 M_w/M_n : 1.05 electronics grade, Polymer Source Inc.) were produced by spin casting a 1.5% w/w solution of PMMA in toluene (99.9% Chromasolv®, Sigma Aldrich) onto freshly cleaved mica (Ted Pella Inc.). The film on mica was scribed into 2 mm x 2 mm pieces with a scalpel. Upon slowly dipping this mica into a Petri dish of water (HPLC grade, Caledon), the film pieces release and float on the surface. These were then caught on Si_3N_4 substrates (1 mm x 1 mm x 75 nm window in a 5 mm x 5 mm Si wafer frame, Norcada Inc.) and annealed at 140°C for one hour at reduced pressure ($\sim 2 \times 10^{-2}$ Torr).

2.2 Scanning transmission X-ray microscopes, resist exposure, development and visualization

Three interferometrically controlled STXMs were employed to pattern the films: STXM 5.3.2.2,¹⁸ and STXM 11.0.2¹⁹ at the Advanced Light Source (ALS), Lawrence Berkeley National Labs (LBNL), and the STXM at beamline 10ID-1²⁰ at the Canadian Light Source (CLS). The methods of STXM operation are described elsewhere.²⁻⁵ Each STXM's zone plate had the same parameters (25 nm outermost zone width, 90 μm central stop, 240 μm diameter) and were fabricated by the Center for X-ray Optics (CXRO) at LBNL. The PMMA samples were affixed to an Al sample plate and loaded into the STXM, which was then evacuated and backfilled with 250 Torr He. Patterning was carried out with 300 eV photons using a pattern generation program in the STXM control software.¹⁸

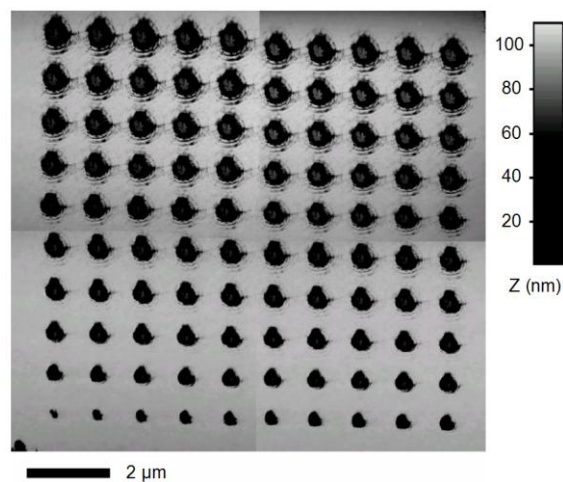


Figure 1. AFM topography image of a developed 100 single pixel exposure pattern in PMMA, made with ALS 11.0.2. Four separate images have been combined.

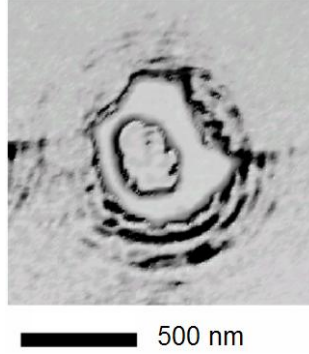


Figure 2. High magnification AFM phase image of the 5000 ms single pixel exposure from the top right corner of figure 1.

We note that it is imperative that the area which is to be patterned not be STXM imaged, either before or after patterning, as even brief imaging (about 1 ms) is enough to cause unintended patterning. The patterned sample is removed from the sample plate, and developed at ambient temperature ($\sim 20^{\circ}\text{C}$) by gently stirring it in a 3:1 solution of 2-propanol ((IPA) 99.5%, Sigma Aldrich) : 4-methyl-2-pentanone (>98.5% ACS reagent grade, Sigma Aldrich) for 30 s, followed immediately by stirring in IPA for 15 s, then drying in ambient air. The developed patterns were then imaged with a Quesant 350 atomic force microscope (AFM) equipped with Budget Sensors Multi75Al probes, operating in non-contact mode at a 0.5 Hz scan rate. For large areas, it was necessary to make several smaller images and combine them to achieve high spatial sampling and to reduce skew.

3. RESULTS

The pattern designed to record the PSF consisted of 100 single pixel exposures, in a 10×10 array, spaced $1 \mu\text{m}$ apart. The dwell time for each exposure increases in 50 ms steps from left to right and bottom to top, from 50 ms in the lower left, up to 5000 ms in the top right. **Figure 1** shows an AFM image of the developed 100 single pixel pattern, made using ALS 11.0.2. As pixel dwell times increase the diameter of the fully removed material becomes larger and larger. Insoluble crosslinked PMMA remains in the central part of the pattern, beginning around the tenth exposure. Many rings appear and expand around the central axis as the exposure time increases. A high resolution AFM phase image of the 5000 ms developed point exposure is shown in **Figure 2** to highlight these details. Clearly the rings tend to be circular but are incomplete. The performance of all three STXMs is diffraction limited (see discussion), therefore one expects an intensity distribution of an Airy pattern⁸ at the focal plane. We have thus recorded a partial Airy pattern.

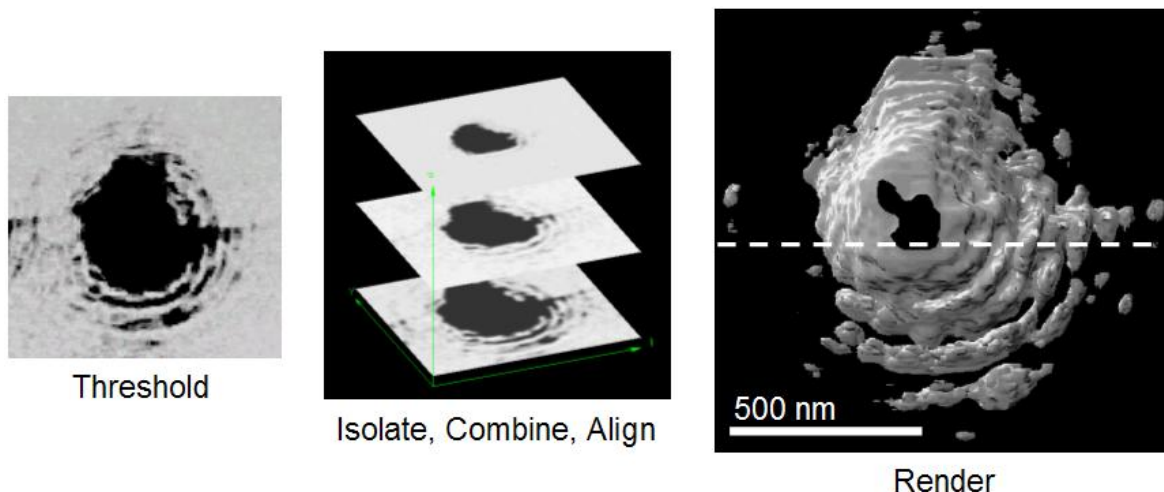


Figure 3. Extracting the full point spread function from the AFM images of developed single pixel exposures. (a) Threshold-ed AFM phase image of the 5000 ms exposure. (b) The procedure used to make the 3D object (c) 3D view, of the outer surface of the stacked AFM images (the z-axis is the image number) made using IDL Slicer²³.

The full PSF was extracted from the AFM images of the developed single pixel patterns in the following way. A threshold was applied to the AFM phase images such that areas with a height less than 80% of the film thickness were made black. One hundred threshold-ed image files were created, one for each single pixel exposure. There is some unintended overlap from adjacent exposures so that, while 1 μm was used in this work, the spacing should be somewhat larger. The subsequent data processing was carried out using aXis2000.²¹ The set of 100 images was converted into an image sequence (stack) and the individual images were then aligned (translational in x and y only) using Fourier transform cross-correlation procedures. The aligned images were then combined into a three dimensional object using IDL Slicer3²² within aXis2000, displayed in **Figure 3**. This surface represents the full PSF of the optical system.

Arbitrary cross sections of the PSF derived from this 3D object yield information equivalent to the common knife edge method, if one performed it over 180 degrees. A horizontal cross section is shown in **Figure 4**. It is difficult to assign the maxima we have recorded. Theoretically the separation between two neighboring rings of an Airy pattern approaches the value $\lambda / 2\text{NA}$.⁸ For our ZP this value is ~ 25 nm. The strongest recorded rings are regularly spaced, but the spacing is 60 ± 10 nm (Figure 4b). The relative intensity of the maxima are also given by theory,⁸ but again we find no definitive agreement. There may be several reasons for this discrepancy (see discussion).

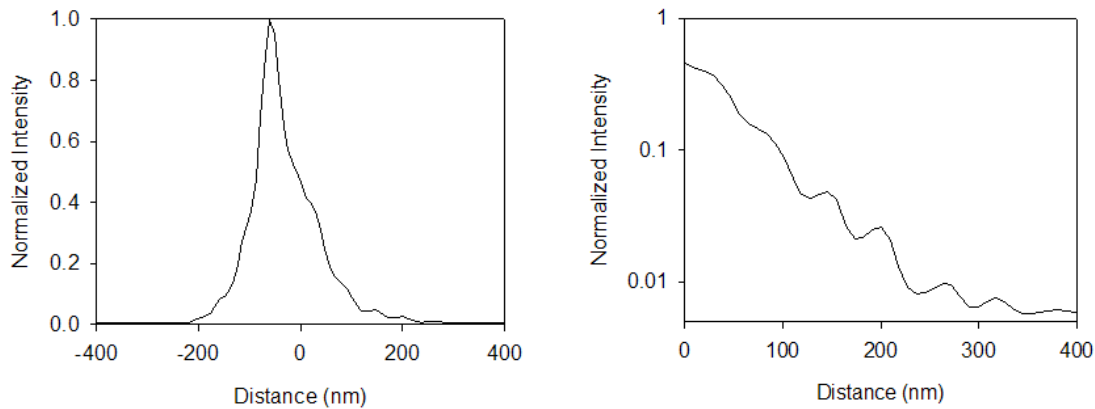


Figure 4. a) Horizontal cross section of the point spread function. The direction and width of the cross section are indicated by the dashed line in figure 3c. b) Intensity on a log scale, showing the maxima and minima.

4. DISCUSSION

A similar method for extracting the PSF of a ZP operating in the visible region has been described by Menon et al.²³, which is also similar to Chang's experimental measurement of the radial exposure intensity distribution introduced by a point source of electrons.¹⁶ In both methods the radial exposure intensity distribution (i.e. PSF) was extracted by plotting normalized intensity (constant/dwell time) versus the radius of the area of removed material. Using our dataset of 100 threshold-ed images, we have found that these methods can not model intensity minima, such as those present in the Airy pattern. In these methods, the presence of a minima would imply that the radius of removed material was observed to decrease with increased dwell time. This is impossible; the radius will only increase or remain the same with increasing dwell time. Our method can measure a minima (figure 4b), making it more accurate than the previous methods. Both prior methods extrapolate the full PSF from data in only one direction, and assume that the PSF is radially symmetric. However, we have shown that this assumption is not always true,¹⁷ and it is certainly not the case for each of the three STXM systems we have investigated. Knife edge measurements are also commonly radially extrapolated. They are challenging at soft X-ray wavelengths because the edge absorber thickness is typically larger than the depth of focus. Our method is not without its own pitfalls. We find it difficult to record the Airy disk (the most intense central spot of the Airy pattern, bordered by the first minima) by our method due to limitations of operating the instrument at full focus and very low exposure doses. The method is also susceptible to artifacts arising from skewed AFM images, and slight misalignment of the threshold-ed images. Despite these challenges we believe the novel method presented here provides unique information about the spatial distribution of radiation intensity in a focal plane with applications extending beyond ZP focused soft X-rays. We are still refining our method, and the findings will be presented in a future paper.

Our efforts are now directed towards understanding why the pattern is not radially symmetric. It was this asymmetry that allowed identification of the exposure spread phenomenon observed in ZP focused soft X-ray patterning as the PSF. The asymmetry is not due to the resist because it is completely reproducible¹⁷ when performed in different photoresists or different regions of the same film. Thus, this pattern must be created by something outside the film, in particular the mechanism of generating the focused spot by the combination of the properties of the ZP and how it is illuminated.

The criteria for diffraction limited focusing of soft X-rays by ZPs such as those used in this work have been given by Jacobsen.²⁴ Assuming the ZP is perfectly fabricated, the ZP is centered relative to the exit slits, and that the ZP and sample are perpendicular to the beam, the basic requirements are that the illumination has sufficient temporal and spatial coherence. For a ZP with n zones the energy resolving power ($\lambda / \Delta\lambda$) necessary to exceed the temporal coherence requirement (sufficient monochromaticity) at a given diffraction order m should be²⁵

$$\frac{\lambda}{\Delta\lambda} \geq n * m \quad (1)$$

The ZPs used in these microscopes have 800 zones, and thus a resolving power of 1000 is more than sufficient to achieve adequate temporal coherence at the first order focal point used to pattern. The ALS 11.0.2 and CLS 10ID-1 undulator based beamlines are routinely operated at a resolving power greater than 3000, while the ALS 5.3.2.2 bend magnet beamline is typically operated with a resolving power of 1500. Thus, the temporal coherence requirement is met by all three STXM beamlines. Spatial coherence is determined by the exit slits, which in each microscope are independently adjustable in x and y , forming an aperture. This aperture diffracts, and the ZP must be fully within the Airy disk emanating from the slits. The exit slit width d corresponding to this limiting condition is

$$d \leq \frac{\lambda}{\sin \theta} \quad (2)$$

where λ is the wavelength (300 eV = 4.13 nm) and θ is the narrow angle of a right triangle formed by the distance from the exit slits to the ZP (1 m for both ALS microscopes, 4 m for CLS 10ID-1) (adjacent), and half the diameter of the ZP (opposite). For our 240 μm ZPs both slits should be $\leq 34 \mu\text{m}$. In all experiments the exit slit widths are set significantly smaller. For the exposures performed at ALS 11.0.2 (figures 1-4) the exit slit sizes were 25 μm x 25 μm , therefore performance should be diffraction limited. As a result the focused intensity of the ZP should produce a symmetric Airy pattern in the focal plane. However we only observe a partial Airy pattern, with significant distortions in specific directions. Even if the ZP and sample were not perpendicular to the beam, that would not explain the roughness of the pattern, since, regardless of such misalignment, the wavefront should be smooth.

We can not yet rule out possible contributions to the PSF asymmetry from non-uniform ZP illumination or other unforeseen instrument problems. The illumination of the zone plate differs considerably among the three STXM microscopes we have examined with this methodology, and depends on the degree of overfill (which is related to the basic design of the beamline optics), and the position and directionality of the electron beam at the source point for the beamline. In the case of ALS 11.0.2, the ZP is uniformly illuminated, as evidenced by the uniformity of the annulus of light in an order sorting aperture scan (**Figure 5**), yet the PSF is not radially symmetric. The ZP illumination of CLS 10ID-1 appears equally uniform, but the PSF is farther away from the expected symmetric Airy pattern. At ALS 5.3.2.2, the illumination was observed to be non-uniform; the PSF here is also farther away from theory. The shape of the PSF of each instrument is unique and very reproducible. In the case of ALS 5.3.2.2 the 100 single pixel exposure measurement was performed several times over a six month period. Although large changes in the illumination of the ZP were observed over this period of time, the overall pattern remained essentially the same, suggesting that the source of the asymmetry lies somewhere after the exit slits and before the sample.

We turn our attention towards the ZP itself. Fabrication of soft X-ray ZPs is at the frontier of electron beam lithography and subsequent plating processes; it is a real challenge to create sub-30 nm ZPs. It may be that the ZPs have aberrations in the placement of zones, out of round, partial collapse of zones in certain regions, etc. These ZPs also have a pseudo-random buttressing system²⁶ to support the zones from collapse during electroplating. The buttressing could modify the ZP focusing from its ideal. There may also be minor contributions from insufficient uniformity in two Si_3N_4 membranes, one which supports the ZP, and another which lies between the exit slits and the ZP that separates the STXM chamber from the ultrahigh vacuum of the beamline.

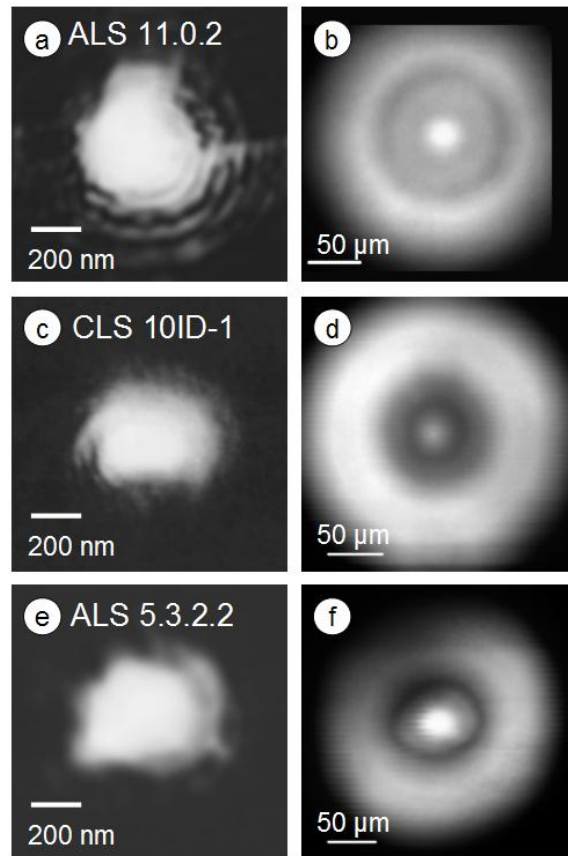


Figure 5. (a) Avg* from ALS 11.0.2 (Avg* is the negative of the average of the 100 aligned threshold-ed AFM images). (b) Illumination of the ZP at ALS 11.0.2 when the 100 point exposure was made. This image was made by (x,y) scanning the 72 μm diameter order sorting aperture (OSA) through a plane between the ZP and its focal point. Parts of the left and upper portion of the X-ray distribution (black areas) were unfortunately not included in the scan. (c) Avg* from CLS 10ID-1. (d) OSA scan for CLS 10ID-1. (e) Avg* from ALS 5.3.2.2. (f) OSA scan for ALS 5.3.2.2.

In order to separate possible effects of non-uniform illumination from those of ZP aberrations, we plan to make single pixel exposure measurements before and after rotating the ZP, with all other factors the same. If the asymmetric pattern is rotated by the same angle as the ZP was rotated, one can conclude that the origin of the asymmetry is the ZP. One difficulty with the three STXMs explored so far is that, once the ZP is rotated, it is possible that it will not be in the same position relative to the illumination, which is problematic because the position of the ZP is not easily adjustable. However, there are other STXMs which are more flexible in this regard, such as PolLux at the Swiss Light Source²⁷, which has a girder mover system that can be used to re-position the ZP in the light path. Also, a new STXM at the ALS (on beamline 5.3.2.1, currently being commissioned) incorporates additional motorized stages for scanning the ZP in the upstream beam. The recently commissioned MAXYMUS STXM at BESSY II has both a girder mover system and the ability to scan the ZP. We propose to carry out the ZP rotation experiment with one or more of these STXMs, in order to re-position the rotated ZP in the same spot relative to the illumination and thus ensure a clean separation of the effects of illumination from those of ZP aberrations on the PSF asymmetry.

Assuming that the asymmetry of the PSF is dominated by ZP aberrations (or that conditions can be adjusted to that end), we will then have developed a tool to characterize the full PSF of ZPs. This could be extremely useful in a number of ways. It could be used to evaluate the quality of different ZPs for soft X-ray focusing. Currently this is done only by examining images of high contrast resolution test patterns such as Siemens star or elbow patterns. Our method could be used to help improve ZP fabrication, by correlating different aspects of the distorted patterns with various process variables. It could also be used to remove image artifacts associated with ZP aberrations, by deconvoluting the PSF. This

approach was used many years ago by Chapman et al.²⁸ to significantly extend the spatial resolution in STXMs and is currently part of the signal processing of ptychography data.²⁹

5. CONCLUSION

We have previously shown that the exposure spread phenomenon observed when patterning with zone plate focused soft X-rays is due to the point spread function of the optical system. In this work we were able to record partial Airy patterns, further strengthening our hypothesis. A method was developed to extract the full point spread function of a sufficiently coherently illuminated zone plate from AFM images of developed single pixel exposures in a photoresist over a range of dwell times. Experiments are underway to separate the effect of illumination from zone plate aberrations, in order to determine precisely the extent to which the recorded pattern reflects the properties of the zone plate.

ACKNOWLEDGEMENTS

This research was supported by NSERC (Canada), the Canada Foundation for Innovation and the Canada Research Chair program. Studies were performed at the Advanced Light Source, beamlines 5.3.2.2 and 11.0.2 (ALS, Berkeley, CA, USA) and the Canadian Light Source, beamline 10ID-1 (CLS, Saskatoon, SK, Canada). We thank Dr. David Kilcoyne (ALS 5.3.2.2), Dr. Jian Wang and Yingshen Lu (CLS 10ID-1) for their support of the STXM facilities. The Advanced Light Source is supported by the Director, Office of Energy Research, Office of Basic Energy Sciences, Materials Sciences Division of the U.S. Department of Energy, under Contract No. DE-AC03-76SF00098. The CLS is supported by NSERC, CIHR, NRC and the University of Saskatchewan.

REFERENCES

- [1] Attwood, D., [Soft X-rays and Extreme Ultraviolet Radiation: Principles and Applications], Cambridge University Press, Cambridge (1999).
- [2] Hawkes, P.W., Spence, J.C.H., [Science of Microscopy], Springer, New York. Chapter 13 (2007)
- [3] Kirz, J., Jacobsen, C., Howells, M., "Soft X-ray microscopes and their biological applications," *Q. Rev. Biophys.* 28, 33-130 (1995).
- [4] Ade, H., Hitchcock, A.P., "NEXAFS microscopy and resonant scattering: Composition and orientation probed in real and reciprocal space," *Polymer* 49, 643-675 (2008).
- [5] Hitchcock, A.P. [Handbook on Nanoscopy], Wiley-VCH, Verlag Gmb-H. Volume I, Chapter XX (in press) (2011)
- [6] Chao, W., Harteneck, B.D., Liddle, J.A., Anderson, E.H., Attwood, D.T., "Soft X-ray microscopy at a spatial resolution better than 15 nm," *Nature* 435, 1210-1213 (2005).
- [7] Chao, W., Kim, J., Rekawa, S., Fischer, P., Anderson, E.H., "Demonstration of 12 nm resolution fresnel zone plate lens based soft X-ray microscopy," *Opt. Express* 17, 17669-17677 (2009).
- [8] Born, M., Wolf, E., [Principles of Optics], Cambridge University Press, Cambridge. pg 436ff (1999)
- [9] Beetz, T., Jacobsen, C., "Soft X-ray radiation-damage studies in PMMA using a cryo-STXM," *J. Synchrotron Rad.* 10, 280-283 (2003).
- [10] Howells, M.R., Beetz, T., Chapman, H.N., Cui, C., Holton, J.M., Jacobsen, C.J., Kirz, J., Lima, E., Marchesini, S., Miao, H., Sayre, D., Shapiro, D.A., Spence, J.C.H., Starodub, D., "An assessment of the resolution limitation due to radiation-damage in X-ray diffraction microscopy," *J. El. Spec. Rel. Phenom.* 170, 4-12 (2009).
- [11] Zhang, X., Jacobsen, C., Lindaas, S., Williams, S., "Exposure strategies for polymethyl methacrylate from in situ x-ray absorption near edge structure spectroscopy," *J. Vac. Sci. Technol. B* 13, 1477-1483 (1995).
- [12] Larciprete, R., Gregoratti, L., Danailov, M., Montekali, R.M., Bonfigli, F., Kiskinova, M., "Direct writing of fluorescent patterns on LiF films by x-ray microprobe," *Appl. Phys. Lett.* 80, 3862-3863 (2002).
- [13] Wang, J., Stöver, H.D.H., Hitchcock, A.P., Tyliczszak, T., "Chemically selective soft X-ray patterning of polymers," *J. Synchrotron Rad.* 14, 181-190 (2007).
- [14] Wang, J., Stöver, H.D.H., Hitchcock, A.P., "Chemically selective soft X-ray direct-write patterning of multilayer polymer films," *J. Phys. Chem. C* 111, 16330-16338 (2007).

- [15] Caster, A.G., Kowarik, S., Schwartzberg, A.M., Leone, S.R., Tivanski, A., Gilles, M.K., "Quantifying reaction spread and x-ray exposure sensitivity in hydrogen silsesquioxane latent resist patterns with x-ray spectromicroscopy," *J. Vac. Sci. Technol. B* 28, 1304-1313 (2010).
- [16] Chang, T.H.P., "Proximity effect in electron-beam lithography," *J. Vac. Sci. Technol.* 12, 1271-1275 (1975).
- [17] Leontowich, A.F.G., Hitchcock, A.P., "Zone plate focused soft X-ray lithography," *Appl. Phys. A* 103, 1-11 (2011).
- [18] Kilcoyne, A.L.D., Tyliczszak, T., Steele, W.F., Fakra, S., Hitchcock, P., Franck, K., Anderson, E., Harteneck, B., Rightor, E.G., Mitchell, G.E., Hitchcock, A.P., Yang, L., Warwick, T., Ade, H., "Interferometer-controlled scanning transmission microscopes at the Advanced Light Source," *J. Synchrotron Rad.* 10, 125-136 (2003).
- [19] Tyliczszak, T., Warwick, T., Kilcoyne, A.L.D., Fakra, S., Shuh, D.K., Yoon, T.H., Brown, G.E.Jr., Andrews, S., Chembrolu, V., Strachan, J., Acremann, Y., "Soft X-ray scanning transmission microscope working in an extended energy range at the Advanced Light Source," *AIP Conf. Proc.* 705, 1356-1359 (2004).
- [20] Kaznatcheev, K.V., Karunakaran, Ch., Lanke, U.D., Urquhart, S.G., Obst, M., Hitchcock, A.P., "Soft X-ray spectromicroscopy beamline at the CLS: Commissioning results," *Nucl. Inst. Meth. A* 582, 96-99 (2007).
- [21] aXis2000 is written in Interactive Data Language (IDL). It is available free for non-commercial use from <http://unicorn.mcmaster.ca/aXis2000.html>
- [22] Carr, D. "Slicer3.pro," in IDL, available from ITT Visual Information Solutions
- [23] Menon, R., Gil, D., Smith, H.I., "Experimental characterization of focusing by high-numerical-aperture zone plates," *J. Opt. Soc. Am. A* 23, 567-571 (2006).
- [24] Jacobsen, C., Williams, S., Anderson, E., Browne, M.T., Buckley, C.J., Kern, D., Kirz, J., Rivers, M., Zhang, X., "Diffraction-limited imaging in a scanning transmission x-ray microscope," *Opt. Comm.* 86, 351-364 (1991).
- [25] Sayre, D., Howells, M., Kirz, J., Rarback, H., [X-Ray Microscopy II], Springer-Verlag, Berlin. 74-78, (1988)
- [26] Olynick, D.L., Harteneck, B.D., Veklerov, E., Tendulkar, M., Liddle, J.A., Kilcoyne, A.L.D., Tyliczszak, T., "25 nm mechanically buttressed high aspect ratio zone plates: Fabrication and performance," *J. Vac. Sci. Technol. B* 22, 3186-3190 (2004).
- [27] Raabe, J., Tzvetkov, G., Flechsig, U., Böge, M., Jaggi, A., Sarafimov, B., Vernooij, M.G.C., Huthwelker, T., Ade, H., Kilcoyne, D., Tyliczszak, T., Fink, R.H., Quitmann, C., "PolLux: A new facility for soft x-ray spectromicroscopy at the Swiss Light Source," *Rev. Sci. Instrum.* 79, 113704 (2008).
- [28] Chapman, H.N., Jacobsen, C., Williams, S., "Applications of a CCD detector in scanning transmission x-ray microscope," *Rev. Sci. Instrum.* 66, 1332-1334 (1995).
- [29] Thibault, P., Dierolf, M., Menzel, A., Bunk, O., David, C., Pfeiffer, F., "High-resolution scanning X-ray diffraction microscopy," *Science* 321, 379-382 (2008).